Synthesis and Characteristics of the Organic Layered Structure Material of $(C_4H_9NH_3)_2Fe_xPb_{1-x}Cl_4$

Su Jin Jung, Ri-Zhu Yin, Eung Ju Oh,† Ung-In Cho, Keu Hong Kim, and Chul Hyun Yo*

Department of Chemistry, Yonsei University, Seoul 120-749, Korea
†Department of Chemistry, Myongji University, Yongin 449-728, Korea
Received September 20, 2000

K_2NiF_4-type organic-based perovskites of the $(C_4H_9NH_3)_2Fe_xPb_{1-x}Cl_4$ (x=0.00, 0.25, 0.50, and 0.75) system have been synthesized using a low-temperature solution method under a flowing argon gas. When stoichiometric butylamine, iron chloride, and lead chloride are mixed, a yellow solution are obtained from slow cooling of 90 to -10 °C. The final product is a plate-like yellow crystal. The X-ray crystallographic analysis has been carried out using XRD in the range of $5^o \leq 2\theta \leq 80^o$. The local symmetry around the absorbing Pb atom of the samples has been determined by the EXAFS spectroscopic study. The crystals assign to orthorhombic system by the XRD analysis. The FT-IR spectra are analyzed in the range of 600 to 3300 cm^{-1}. DSC and TGA are measured to detect thermal stability between 30 and 300 °C. Two endothermic peaks are detected in all samples. The electrical conductivity has been measured using the four-probes technique for the $(C_4H_9NH_3)_2Fe_xPb_{1-x}Cl_4$ system in 300-460 K. Photoluminescence phenomenon was also investigated at room-temperature.

Keywords : Organic layered, Local symmetry, EXAFS, Electrical conductivity, Photoluminescence.

Introduction

Recently, the divalent transition metal halide members of the organic-inorganic perovskite family have been studied and have generated considerable interest as self-assembling multi-quantum-well structure.[1-6] Layered perovskite-type compounds have naturally formed the quantum-well structure consisting of a metal halide semiconductor sheet sandwiched between organic insulator layers.

Due to the low dimensionality of these compounds, the exciton has a large binding energy, which enables strong photoluminescence even at room temperature.[7-9] Thus the materials are sufficient to offer applications in emitter materials in electroluminescent devices.[10,11]

While inorganic materials offer the potential for high carrier density, mobility, and substantial thermal stability, organic materials provide virtually unlimited flexibility to choose molecules for varying length, width, and polarizability. The inorganic component forms an extended framework bound by strong covalent or ionic interaction to provide high carrier mobilities. The organic component forms by weak van der Waals interaction to offer low-cost and low-temperature processes.

In the present study, the solid solution of the $(C_4H_9NH_3)_2Fe_xPb_{1-x}Cl_4$ (x=0.00, 0.25, 0.50, and 0.75) system have been synthesized and characterized by X-ray diffraction, thermal, electrical, and optical studies. The effect of the replacement of divalent metal on the formation of two dimensional materials has also been investigated.

Experimental Section

Butyl amine ($C_4H_9NH_3$), hydrochloric acid (HCl) (aqueous solution 35%), iron chloride ($FeCl_2$), and lead chloride ($PbCl_2$) are commercially available. The compounds of the $(C_4H_9NH_3)_2Fe_xPb_{1-x}Cl_4$ (x=0.00, 0.25, 0.50, and 0.75) system have been synthesized by reacting the $C_4H_9NH_3$, $FeCl_2$ and $PbCl_2$ mixture in the HCl solution with flowing Ar gas. The mixed starting materials are heated to 90 °C and cooled slowly to -10 °C. The sheet like crystals of layered lead compound are white, while those of the iron compound are yellow.

X-ray diffraction spectra of the powder samples are recorded up to 80^o of 2θ value at room temperature by Rigaku X-ray diffractometer with Ni-filtered Cu-Kα (λ = 1.5406 Å) radiation at 40 kV and 35 mA.

Infrared spectra are recorded on the range of 1000 to 3300 cm^{-1} using Bruker IFS66 spectrometer with pressed KBr pellets. Coordination number, local structure, Debye-Waller factor and bond distance for the samples have been determined by measuring extended X-ray absorption fine structure (EXAFS) in Pohang Light Source.

Differential scanning calorimetry (DSC) and thermogravimetric analysis (TGA) measurements are carried out in the temperature range of 30 to 300 °C to examine the thermal stability and phase transition of the powder compounds.

Electrical conductivity measurements of a pressed pellet sample have been carried out using a four-probes method in the temperature range of 300 to 460 K. The conductivity measurements are taken at 5 °C intervals.

Photoluminescence (PL) spectra are obtained at room temperature by using a Xe lamp as a excitation source for the PL measurement (HITACHI F-4500 spectrophotometer). The exciting wavelength has ranged from 200 to 330 nm in which optimum one is 280 nm.

Results and Discussion

X-ray Diffraction. X-ray diffraction patterns of the

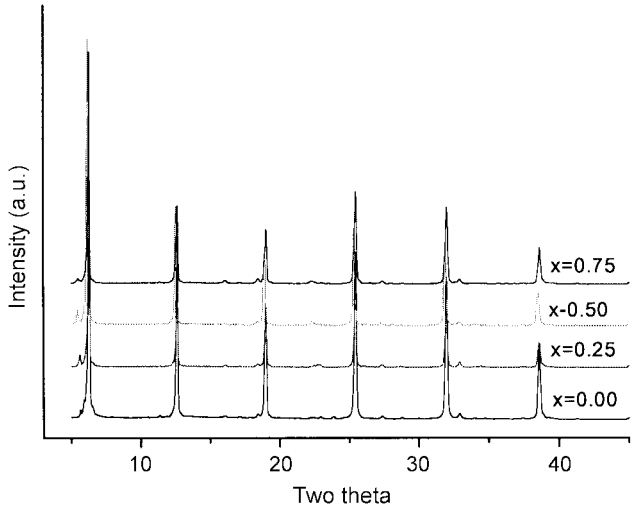

Figure 1. Powder XRD patterns for the $(C_4H_9NH_3)_2Fe_xPb_{1-x}Cl_4$ system at room temperature.

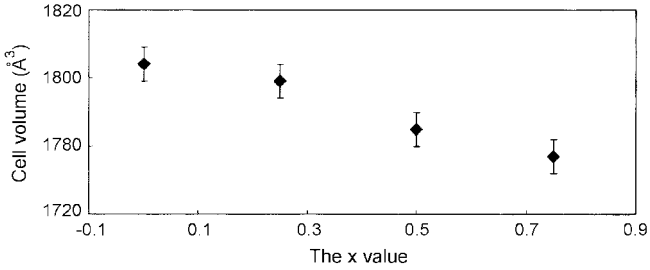

Figure 2. Cell volume of the $(C_4H_9NH_3)_2Fe_xPb_{1-x}Cl_4$ system as a function of the x value.

$(C_4H_9NH_3)_2Fe_xPb_{1-x}Cl_4$ (x=0.00, 0.25, 0.50, and 0.75) system have been observed for organic-inorganic perovskites as shown in Figure 1. A (0 0 l) reflection corresponds to an interlayer distance of 14.06 Å separating the inorganic sheets are clearly observed and shows good solid solution for the layered compounds. The X-ray crystallographic structure of all compounds assigns to an orthorhombic system, which is refined by the least-square method. From the XRD patterns analysis, lattice volumes decrease with increasing x value of $(C_4H_9NH_3)_2Fe_xPb_{1-x}Cl_4$ as shown in Figure 2 since small iron atom substitutes the larger Pb atom. The lattice parameters, cell volume of all compounds are listed in Table 1. The interlayer distance between inorganic sheets is not affected by the substituted iron ions since the length of organic layer is the main factor of the interlayer distance.

Table 1. Lattice parameters and cell volume for the $(C_4H_9NH_3)_2Fe_xPb_{1-x}Cl_4$ system

Composition (x)	Lattice parameter (Å)			Cell volume (Å^3)
	a	b	c	
0.00	8.288 ± 0.002	7.797 ± 0.002	27.98 ± 0.04	1808
0.25	8.156 ± 0.003	7.884 ± 0.003	27.98 ± 0.05	1799
0.50	8.185 ± 0.004	7.781 ± 0.008	28.04 ± 0.02	1785
0.75	8.361 ± 0.003	7.600 ± 0.003	27.98 ± 0.01	1777

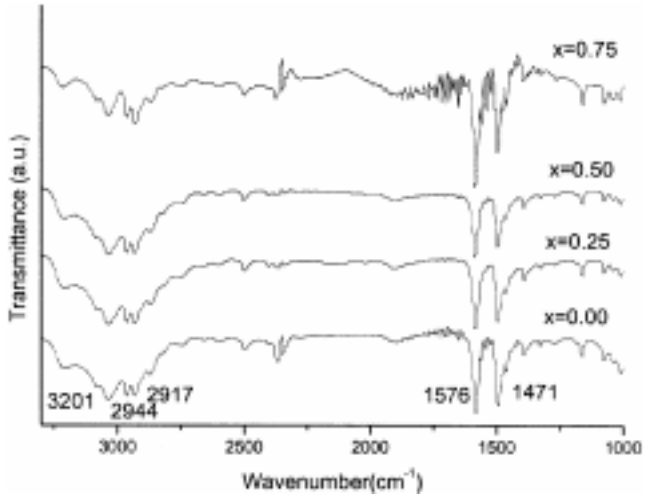

Figure 3. Infrared transmission spectra of the $(C_4H_9NH_3)_2Fe_xPb_{1-x}Cl_4$ system.

FT-IR Spectroscopy. FT-IR spectra of the $(C_4H_9NH_3)_2Fe_xPb_{1-x}Cl_4$ (x=0.00, 0.25, 0.50, and 0.75) system between 1000 and 3300 cm^{-1} shows the structure of the butylammonium chains as shown in Figure 3. The symmetric bending mode of CH_3 is shown at 1380 cm^{-1} and those of CH_3 and CH_2 are shown at 1471 cm^{-1}. The asymmetric and symmetric stretching modes of CH_2 are shown at 2917 and 2850 cm^{-1}, respectively. The FT-IR spectra do not show any significant change on the *n*-butylamine. This means that the general structure of organic layers is conserved. It also represents that the synthesized compounds have low dimensionality.

EXAFS Spectroscopy. EXAFS spectroscopic analysis of the $(C_4H_9NH_3)_2Fe_xPb_{1-x}Cl_4$ (x=0.00, 0.25, 0.50, and 0.75) system represents the local structure around the absorbing Pb atom. Pb L_{III}-edge EXAFS data have been fitted by using a nonlinear fitting method and computer code FEFF6. Figure 4 shows the k^1 weighted Pb L_{III}-edge EXAFS spectra of the $(C_4H_9NH_3)_2Fe_xPb_{1-x}Cl_4$ system in k-space. Bond lengths between Pb and Cl atoms and structural parameters are determined from the EXAFS fitting as shown in Figure 4 and Table 2. Bond lengths between octahedral coordinated chloride ions and the Pb atom are different values in x, y, and z axes. In general, the bond lengths between the Pb and Cl atoms are shorten with the increasing x value, which shows a good relation with the result of the conductivity measurements. Lone-pair electrons of Pb(II) and Fe(II) atoms in outer shells prefer to distort the lattice structure. The shorter Pb-Cl bond length is also in agreement with the lattice volume decreasing. The first shell between 1 and 4 Å is fitted in Pb-Cl pair as shown in Figure 5.

Thermal Analysis. Due to the organic cations of the samples, the materials are expected to decompose at relatively low temperature. Figure 6 shows the thermogravimetric analysis (TGA) and differential scanning calorimetry (DSC) curves for the $(C_4H_9NH_3)_2Fe_xPb_{1-x}Cl_4$ system. The samples begin to slowly lose the weight at the temperature

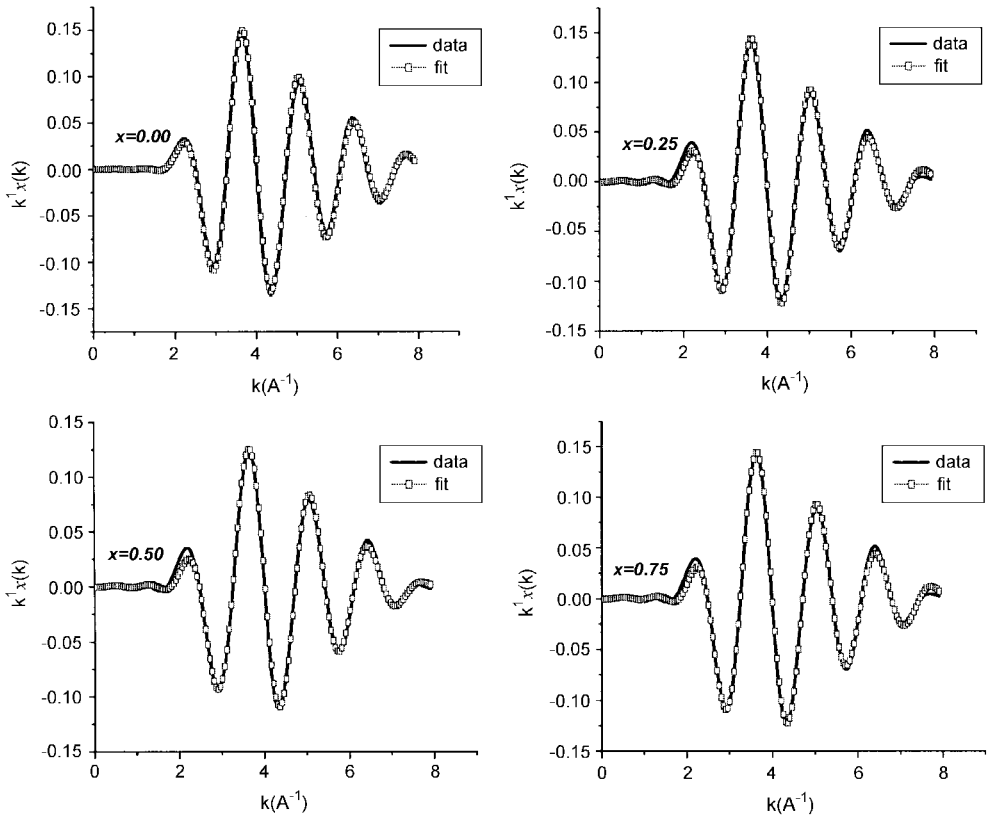

Figure 4. Pb L_{III}-edge EXAFS $k^1\chi(k)$ spectra the $(C_4H_9NH_3)_2Fe_xPb_{1-x}Cl_4$ system.

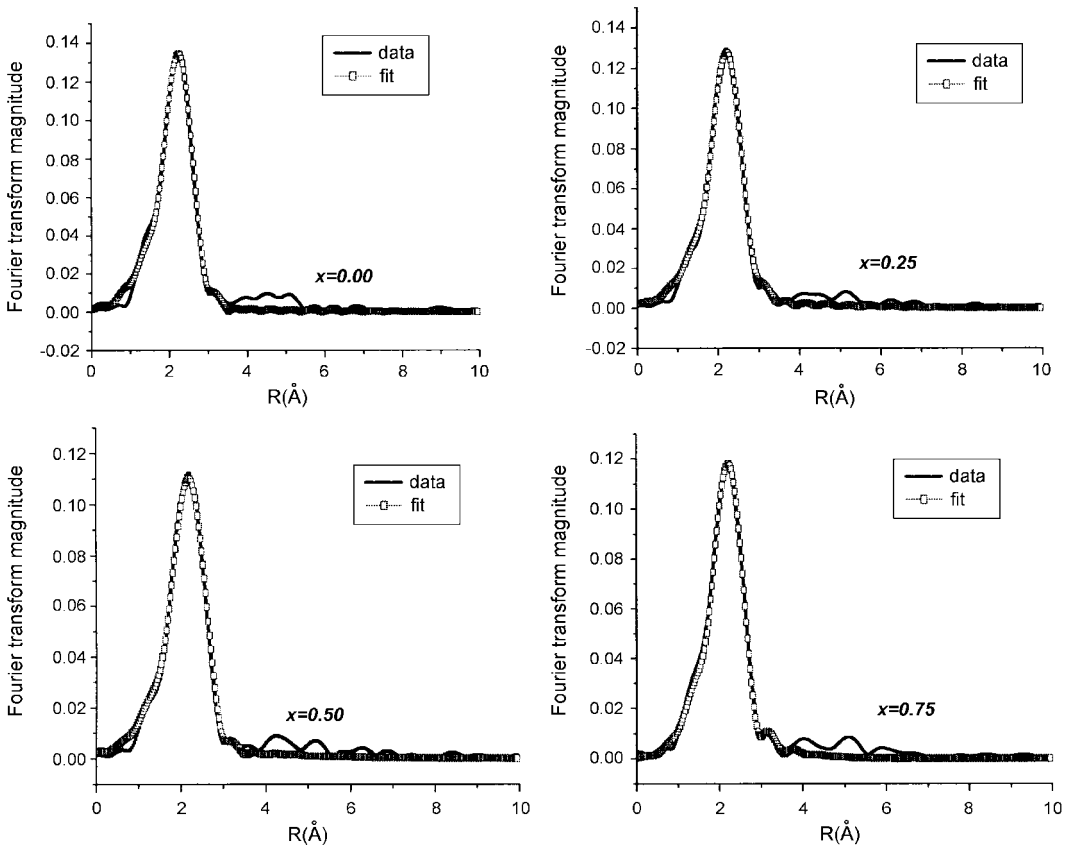

Figure 5. Fourier transform magnitude of Pb L_{III}-edge EXAFS spectra for the $(C_4H_9NH_3)_2Fe_xPb_{1-x}Cl_4$ system.

Table 2. Structural parameters from Pb L_{III}-edge EXAFS spectra for the $(C_4H_9NH_3)_2Fe_xPb_{1-x}Cl_4$ system

Composition (x)	PbCl(I)			PbCl(II)			PbCl(III)			R^d factor for fit
	N^a	R^b (Å)	σ^c	N	R (Å)	σ	N	R (Å)	σ	
0.00	2	2.891(1)	0.0083(3)	2	2.778(1)	0.0081(3)	2	3.002(1)	0.0081(3)	0.007
0.25	2	2.850(2)	0.0074(3)	2	2.754(2)	0.0077(3)	2	3.000(2)	0.0075(3)	0.006
0.50	2	2.838(4)	0.0031(4)	2	2.712(4)	0.0039(4)	2	2.982(4)	0.0023(4)	0.006
0.75	2	2.767(7)	0.0066(5)	2	2.923(7)	0.0052(5)	2	2.960(7)	0.0048(5)	0.009

[a]N: Coordination number, [b]R: bond distance, [c]σ: Debye-Waller factor, and [d]R: Goodness of fit.

of about 200 °C as shown in the TGA curve. Two endothermic peaks are also detected in the DSC curve. The first transition takes place primarily by order-disorder transition of the butylammonium cation within the organic layer. The second transition corresponds to a complete decomposition at the temperature above 200 °C. The transition temperature, enthalpy change, and entropy change of the $(C_4H_9NH_3)_2Fe_xPb_{1-x}Cl_4$ system is listed in Table 3. Since the organic layer has only the phase transition, ΔS_t value is determined by the relationship of $\Delta S_t = \Delta H_t/T_t$.

Table 3. The transition temperature, enthalpy change, and entropy change of the $(C_4H_9NH_3)_2Fe_xPb_{1-x}Cl_4$ system

Composition (x)	T_t (°C)	ΔH_t	ΔS_t
0.00	56.39	2.931	8.90
0.25	55.81	2.860	8.70
0.50	55.34	2.800	8.52
0.75	55.23	27.52	8.52

Electrical Conductivity. The electrical conductivities have been measured by the four-probes technique for the pressed pellet samples of the $(C_4H_9NH_3)_2Fe_xPb_{1-x}Cl_4$ system under the air pressure as shown in Figure 7. Although the conductivities of all compounds at room temperature have shown an insulating value, the conductivities of the compounds are increased with the temperature, which represent typical semiconducting properties at about 450 K. The conductivity also increases as the x-value increases. Since the Fe atom has unpaired electrons in a d orbital, the electron transference is easier than that in the Pb atom. The shorter Pb to Cl length also consists to increasing conductivity of the compounds. The delicate conductivities may be related to a structural distortion within the butylammonium cation ordering in the structure. Since the sample heated above 470 K shows some decomposition, the conductivity measurements are limited in the temperature range of 300 to 460 K.

Photoluminescence. Organic-inorganic layered perovskites of the $(C_4H_9NH_3)_2Fe_xPb_{1-x}Cl_4$ system exhibit a sharp photoluminescence emission peak at room temperature as shown

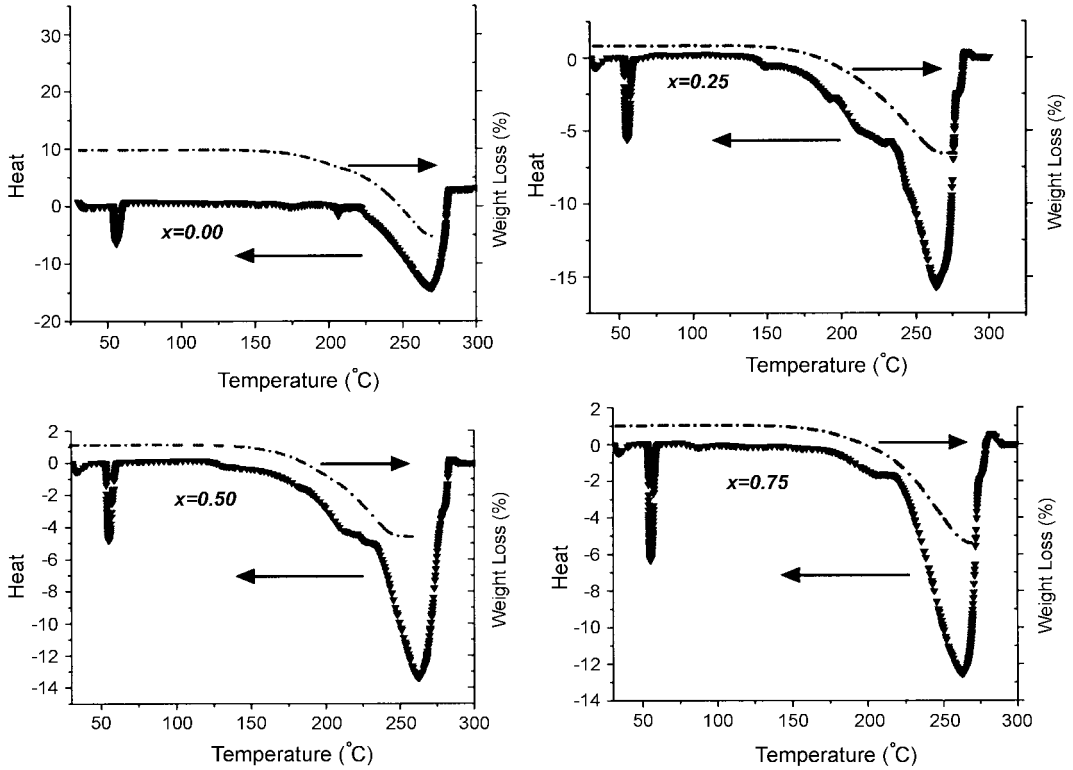

Figure 6. The DSC and TGA patterns of the $(C_4H_9NH_3)_2Fe_xPb_{1-x}Cl_4$ system.

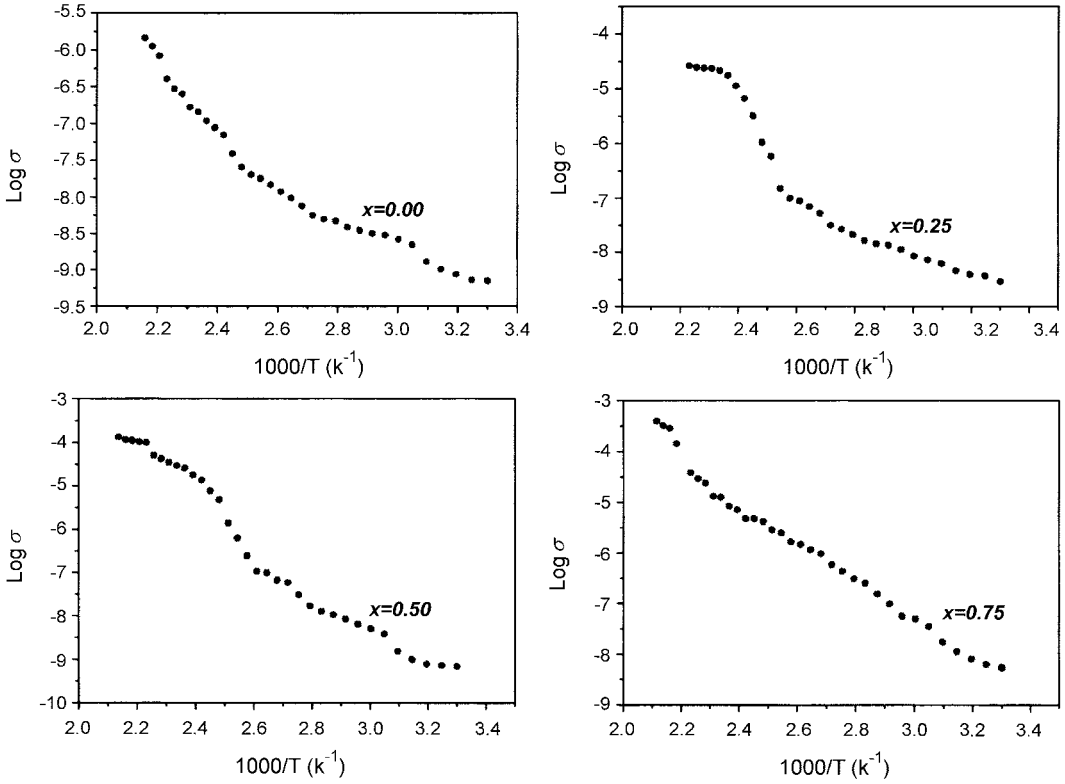

Figure 7. The plot of log electrical conductivity *vs* 1000/T for the $(C_4H_9NH_3)_2Fe_xPb_{1-x}Cl_4$ system.

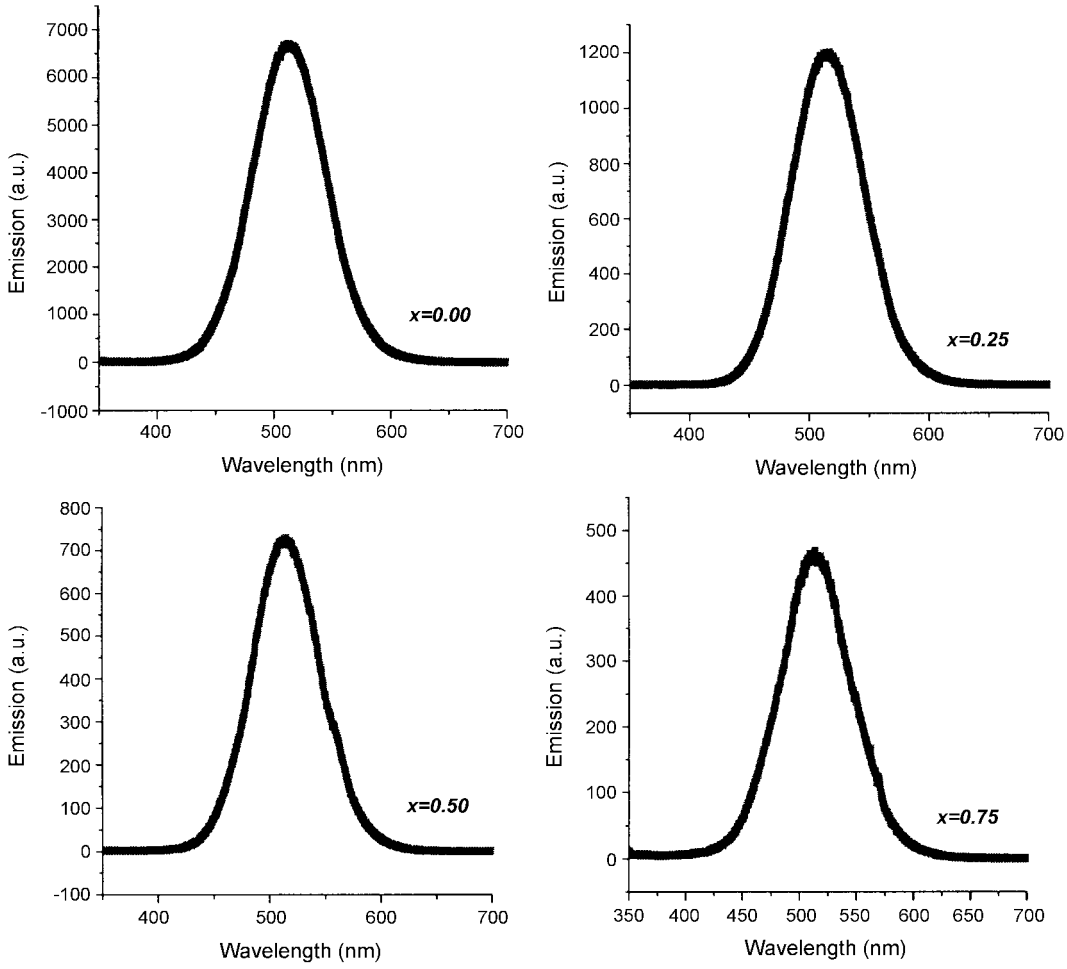

Figure 8. The photoluminescence spectra of the $(C_4H_9NH_3)_2Fe_xPb_{1-x}Cl_4$ system at 280 nm excitation.

in Figure 8. The luminescence originates from the electronic transitions within the inorganic layer. When the compounds are excited at wavelength of 200 nm to 330 nm, strong and sharp peaks have been observed at 516, 515.4, 515, and 513 nm for the compositions of x=0.00, 0.25, 0.50, and 0.75 in the $(C_4H_9NH_3)_2Fe_xPb_{1-x}Cl_4$ system, respectively. The emission peak positions are not dependent on the excitation wavelength, even if some differences in the peak intensities are observed. Since the emission peak arises from an excitation state in the inorganic sheets of the layered perovskite structure, the delicate peak changes are possible due to structural distortion in the compounds. However, the emission peak does not change by the x-value. Thus, PL main emission peaks originate from the Pb inner band between Pb(6p) and Pb(6s) bands. The PL peaks show an independent behavior from Cl ion orbital mixing.

Conclusion

In the present study, a low-temperature synthetic technique has been described for the $(C_4H_9NH_3)_2Fe_xPb_{1-x}Cl_4$ system. All the solid solutions assign to orthorhombic structure at room temperature. From EXAFS spectroscopic analysis, the bond length of Pb-Cl is decreased with increasing x value. The materials have shown weak semiconducting properties in the temperature range of 300 to 460 K. All the compounds have shown the relative stability in an inert atmosphere up to about 200 ^oC and also shown the sharp and strong PL emission peaks.

Acknowledgment. The authors wish to acknowledge the financial support of the Korea Research Foundation made in the program year of 1998 (98-015-D00156).

References

1. Tabuchi, Y.; Asai, K.; Rikukawa, M.; Sanui, K.; Ishigure, K. *J. Physics and Chem. of Solids* **2000**, *61*, 837.
2. Lee, S. J.; Kim, G. Y.; Oh, E. J.; Kim, K. H.; Yo, C. H. *Bull. Korean Chem. Soc*. **2000**, *21*(3), 317.
3. Wang, W.; Chen, X.; Efrima, S. *Chem. Mater.* **1999**, *11*, 1883.
4. Kagan, C. R.; Mitzi, D. B.; Dimitrakopoulos, C. D. *Science* **1999**, *286*(29), 945.
5. Yin, R. Z.; Yo, C. H. *Bull. Korean Chem. Soc.* **1998**, *19*(9), 947.
6. Liang, K.; Mitzi, D. B. *Chem. Mater.* **1998**, *10*, 403.
7. Mitzi, D. B.; Liang, K. *Chem. Mater.* **1997**, *9*, 2990.
8. Mitzi, D. B.; Liang, K. *J. Solid State Chem.* **1997**, *134*, 376.
9. Mitzi, D. B. *Chem. Mater.* **1996**, *8*, 791.
10. Mitzi, D. B.; Feild, C. A.; Schlesinger, Z. *J. Solid State Chem*. **1995**, *114*, 159.
11. Mitzi, D. B.; Feild, C. A. *Nature* **1994**, *369*(9), 467.